Technical Reports

Simultaneous observation of Pol II and potato spindle tuber viroid RNA in the nucleus by combining immunofluorescence and RNA in situ hybridization

Junfei Ma[1†*], Yunhan Wang[2†], Svetlana Y. Folimonova[1,2], Bin Liu[3], Ying Wang[1,2*]

1 Department of Plant Pathology, University of Florida, Gainesville, FL 32611, USA
2 Plant Molecular and Cell Biology Program, University of Florida, Gainesville, FL, USA
3 Food Science and Human Nutrition Department, University of Florida, FL, USA

[†] These authors contributed equally to the work.
*Correspondence: Junfei Ma and Ying Wang
Email: junfeima@ufl.edu (JM) and ying.wang1@ufl.edu (YW)

Keywords

viroid, RNA Fluorescence *in situ* hybridization (FISH), Immunofluorescence (IF), RNA-protein co-localization, RNA polymerase II (Pol II)

Abstract

RNA comprises a versatile group of biomolecules that play diverse roles in a wide range of biological processes. From synthesis to degradation, RNAs interact with cognate proteins that assist in processes such as transcription, splicing, modification, trafficking, and the execution of their functions. While numerous valuable techniques exist to study RNA-protein interactions, observing RNAs and their associated proteins simultaneously within cells remains a challenge, despite its potential to provide deeper insights into RNA-protein interactions. In this study, we adapted a modified immunofluorescence (IF) assay combined with RNA fluorescence in situ hybridization (FISH) to successfully visualize the colocalization of potato spindle tuber viroid with RNA polymerase II in the nucleus. This new method that combines IF and FISH will facilitate future studies on RNA and protein colocalization in various plant systems.

Introduction

Mounting evidence has highlighted the essential roles of diverse classes of RNAs across a wide range of biological processes (Sharp, 2009). From transcription to decay, RNAs interact with specific RNA-binding proteins, and these interactions often correlate with distinct biological functions (Street et al., 2024). In certain cases, RNA-protein complexes organize into membrane-less organelles via liquid-liquid phase separation (Miao, Chodasiewicz, & Fang, 2024). Examples include Processing bodies and Stress Granules involved in mRNA turnover or storage (Chantarachot & Bailey-Serres, 2018), SERRATE-driven dicing bodies in microRNA processing (Xie et al., 2021), and FLL2-promoted phase separation of polyadenylation complexes for mRNA 3' end processing (Fang et al., 2019). Although tools such as RNA immunoprecipitation and gel electrophoresis mobility shift assays are valuable for studying RNA-protein interactions, observing RNA subcellular localization or simultaneously visualizing specific RNAs with their associated proteins in cells remains challenging, hindering the understanding of RNA-protein dynamics in the context of cell biology.

The MS2-MCP system enables live-cell imaging of RNAs by using MS2-binding coat proteins (MCP) tagged with green fluorescent protein (GFP) to recognize RNAs fused with MS2 hairpins (Syed & Lim, 2024). By tracking MSP-fused GFP fluorescence, RNA subcellular localization can be observed in living cells with high specificity and temporal resolution. RNA-binding proteins can be co-visualized by tagging them with fluorescent proteins other than GFP. In addition to the MS2-MCP system, RNA fluorescence aptamers also allow visualization of fusion RNAs in living cells (Sachdeva, Garg, Godding, Way, & Silver, 2014). However, both systems pose a risk of disrupting RNA overall structures and functions. For example, any insertion in the viroid RNA genome can lead to a loss of infectivity, limiting the applications of these methods to certain RNAs.

Observing proteins and RNAs in chemically fixed cells can provide insights into their subcellular dynamics. Immunofluorescence (IF) detects specific proteins, while RNA in situ hybridization (FISH) reveals RNA subcellular localization patterns. The development of single-molecule RNA FISH (smFISH) enables the quantitative observation of mRNAs, but it requires dozens of short, specific oligos (17-22 nt) and may not be suitable for short RNAs or those with limited unique sequences (Duncan, Johansson, & Ding, 2023).

Traditional IF and FISH are often incompatible, as the high-temperature treatment and formamide used in FISH denature antibodies, hindering protein detection (Meyer, Garzia, & Tuschl, 2017). Recent protocols offer modifications to address this issue by adjusting formamide concentration and other conditions (B. Ma & Tanese, 2013; Meng, Zhao, & Lao, 2018; Meyer et al., 2017), but performing IF after FISH or smFISH still remains difficult. In some cases, fluorescent proteins (FPs) can retain fluorescence to outline protein subcellular localization after RNA FISH steps (Duncan et al., 2023; Huang, Guillotin, Rahni, Birnbaum, & Wagner, 2023; Zhao, Fonseca, Meschichi, Sicard, & Rosa, 2023), but this approach is mostly limited to observing protein colocalized with cytosolic RNAs. For nuclear RNAs, high temperatures and stringent treatments in the corresponding FISH protocols can cause FPs to lose fluorescence (Jolly, Mongelard, Robert-Nicoud, & Vourc'h, 1997; Qi & Ding, 2003; Yokoyama, Ogawa, Nozu, & Hashimoto, 1990).

Our goal is to understand viroid-host interactions at cellular and subcellular levels. Viroids are single-stranded, circular noncoding RNA pathogens that primarily infect crops (J. Ma, Dissanayaka Mudiyanselage, Hao, & Wang, 2023; Ortola & Daros, 2023). There are two viroid families, *Pospiviroidae* and *Avsunviroidae*. Members of *Pospiviroidae* replicate in the nucleus using RNA polymerase II (Pol II)(Wang, 2021). Unlike the well-known 12-subunit Pol II, a modified Pol II with 6-7 subunits transcribes the potato spindle tuber viroid (PSTVd) RNA (Dissanayaka Mudiyanselage et al., 2022), assisted by an RNA-specific transcription factor (TFIIIA-7ZF)(Dissanayaka Mudiyanselage et al., 2022; Wang et al., 2016). Despite the progress, the detailed subcellular localization and pattern of Pol II transcription on PSTVd RNA remain unclear.

To address this, we developed a new strategy that combines IF and FISH to simultaneously detect PSTVd RNA and the largest Pol II subunit (RPB1). This approach is straightforward, does not require extensive cloning or transgenic plants (if a specific primary antibody is available), and reliably detects RNAs and proteins in the nucleus. Using this method, we observed the nuclear distribution patterns of Pol II (represented by RPB1) and PSTVd sense-strand RNA. This technique will be valuable for studying various nuclear-localized noncoding RNAs and their associated proteins, especially those involved in liquid-liquid phase separation across diverse biological processes.

Results

An alternative immunofluorescence (IF) approach

To understand viroid replication in cells, we aimed to observe the subcellular localization of Pol II and potato spindle tuber viroid (PSTVd). However, our initial attempts were unsuccessful due to the technical challenges of combining immunofluorescence with RNA in situ hybridization. Inspired by a recent study on RNase L-induced bodies that directly incubate antibodies with culture cells (Watkins & Burke, 2024), we hypothesized that incubating antibodies directly with protoplasts could be an effective alternative IF method.

We tested this approach by observing GFP protein localization in the *Nicotiana benthamiana* 16C line, which expresses a GFP5 variant with an ER localization signal (Philips et al., 2017). Figure 1 shows the GFP fluorescence signal in live protoplasts, as well as in cells incubated with antibodies, with and without chemical fixation. As previously reported, polyclonal antibody binding reduced fluorescence of GFP to almost undetectable (Kubala, Kovtun, Alexandrov, & Collins, 2010; Schneider, Sych, Eggeling, & Sezgin, 2021). Nevertheless, signals from the Alexa Fluor594-conjugated secondary antibody accurately highlighted GFP localization, regardless of fixation, demonstrating that directly incubating antibodies with protoplasts can serve as an alternative IF technique.

Optimizing RNA FISH protocol for detecting RNA in the nucleus

Next, we sought to detect PSTVd RNA in fixed cells. Due to PSTVd's short length (359 nt), designing dozens of oligo probes, as required in some single-molecule RNA FISH protocols, was challenging. Instead, we used traditional *in vitro* transcription method to generate RNA oligos.

The key factor was optimizing probe size. We designed probes around 100 nt to facilitate nuclear entry. Each probe contained approximately 25-30 AlexaFluor488-labeled UTPs, and we used two probes, achieving 54 labeled UTPs per PSTVd RNA to enhance the signal-to-background ratio. We tested two methods reported in previous RNA FISH experiments that observed nuclear PSTVd accumulation. Interestingly, combining the penetration steps from both protocols yielded better, more consistent

results (Figure 2). PSTVd displayed a unique distribution pattern, with dominant signals near the nucleolar region, as indicated by the hollow DAPI staining (Figure 2). This PSTVd RNA condensate pattern is consistent with previous reports (Qi & Ding, 2002, 2003).

A new strategy combining IF and FISH to observe RNA-protein simultaneously

Building on the success of our alternative IF and RNA FISH methods, we developed a combined IF-FISH protocol to observe proteins and RNA simultaneously in cells (Figure 3). This strategy involves generating protoplasts from leaves, followed by incubating cells overnight at 4°C with primary antibodies against target proteins. After brief washes, cells are incubated with fluorescence-labeled secondary antibodies. The IF process is followed by cell fixation, permeabilization, blocking, hybridization, and finally, observation. The entire procedure can be completed in four days.

The new IF-FISH method helps direct observation of the cellular sites of Pol II transcription on PSTVd sense-strand RNA

Using this system, we aimed to understand the subcellular distribution of Pol II and PSTVd RNA. Although PSTVd replication depends on Pol II activity, the exact nuclear distribution pattern involved in PSTVd RNA-templated transcription remain unclear. We used the well-known 8WG16 monoclonal antibody to detect Pol II localization via its largest subunit (RPB1). Our previous studies confirmed that 8WG16 specifically recognizes RPB1 in immunoblots using total protein extracts from *N. benthamiana* leaves (Wang et al., 2016). As shown in Figure 4A, there is no fluorescence signal from Alexa Fluor594-conjugated secondary antibody in samples which we did not add primary antibody, demonstrating the specificity in detecting target protein. Similarly, PSTVd specific riboprobe did not give any signal in non-infected cells, again support the specific detection in FISH experiment.

In a selected image from a Z-stack series (Figure 4B), we found that some of the RPB1 and PSTVd colocalized loci are surrounding bot not overlapping with the highly enriched PSTVd RNA condensate. There are more colocalized loci spreading in nucleoplasm. This pattern demonstrates that there is no major locus for Pol II to transcribe the template of PSTVd sense-strand RNA. Rather, the transcription occurs in multiple loci

mainly in the nucleoplasm.

Discussion

By combining IF and RNA-FISH, we successfully achieved the simultaneous observation of RNA and protein in the nucleus of plant cells. This approach eliminates the need for extensive cloning, as required in the MS2–MCP system, or the generation of transgenic plants when a specific primary antibody is available. Notably, our protocol is particularly effective for detecting RNAs in the nucleus, which has proven challenging based on both literature and our experience. Additionally, this method allows the direct visualization of proteins and RNAs in their native state without ectopic expression, making it a robust and straightforward approach for plant cell biology studies.

Compared to smFISH, our probe design strategy offers an advantage in detecting relatively short RNAs that are insufficient in length for designing multiple oligos. While we used a long probe (~100 nt) to detect PSTVd sense-strand RNA, our method could be adapted in combination with smFISH to detect endogenous mRNAs. Moreover, multiple proteins and/or RNAs can be observed within the same cells by utilizing various AlexaFluor dyes, allowing different targets to be marked with distinct colors. This flexibility enables researchers to adapt the method to address a range of biological questions.

Recent studies have increasingly highlighted the importance of dynamic RNA organization and their associated factors within the cellular environment, particularly in the context of phase separation across diverse biological processes (Miao et al., 2024). However, most knowledge has been derived either from methods lacking cellular context (e.g., RIP-Seq) or indirectly by observing either protein or RNA subcellular localization alone. Our method provides a means to directly investigate the dynamic interactions between RNA and protein in cells, offering a valuable tool for future research.

By using our method, we now understand that Pol II transcribing sense-strand of PSTVd in multiple loci in the nucleoplasm. Since Pol II transcription loci do not overlap with the major PSTVd RNA condensate, this result excludes the PSTVd RNA condensate as the transcription site. Rather, the PSTVd RNA condensate is possibly the organized place for processing (e.g., cleavage, ligation, etc) after transcription. We believe this method is suitable to study the colocalization of RNA and protein, particularly for those

that occurred in the nucleus.

Materials and methods

Plant Growth and Protoplast Preparation

Nicotiana benthamiana (wild type and line 16C) were grown in a growth shelf at 25 °C with a 16-hour light and 8-hour dark cycle. PSTVd-infected plants were verified by RNA gel blots as described previously (Takeda, Zirbel, Leontis, Wang, & Ding, 2018). Protoplasts were isolated from the 4th to 6th leaves of the plants by following a published protocol with slight modifications (Jiang, Ma, Liu, & Wang, 2019). Briefly, leaves were digested with 3% cellulose (Onozuka Yakult Pharmaceutical IND., Tokyo, Japan) and 0.8% macerase (MilliporeSigma, Burlington, MA, USA) in protoplast digestion buffer (0.4 M mannitol, 20 mM KCl, 20 mM MES, 10 mM $CaCl_2$, 0.1% BSA, 5 mM β-mercaptoethanol, pH 5.7). The lower epidermis layer of the leaves was removed by tapes before digestion. After 1 hr of digestion, the protoplasts were pelleted by centrifugation at 150× *g* for 1 min. The pelleted protoplasts were then washed sequentially with W5 buffer (5 mM MES, 154 mM NaCl, 125 mM $CaCl_2$, 5 mM KCl, pH 5.7) at room temperature. Finally, the protoplasts were incubated in IF buffer (0.5 M mannitol, 20 mM MES, pH 5.7, 20 mM KCl, 1% BSA, 0.1% Tween-20) before adding primary antibodies.

Immunofluorescence (IF)

The IF method was adapted from a study on *in vivo* antibody uptake (Watkins & Burke, 2024). Freshly prepared protoplasts were incubated overnight at 4°C with primary antibodies diluted 1:500 in IF buffer (protoplast digestion buffer with 1% BSA and 0.1% Tween 20). After primary antibody incubation, protoplasts were washed three times with IF buffer with a 10 min interval. Secondary antibodies were added in IF buffer with a 1:50 dilution and incubated at room temperature for 3 hr. The protoplasts were washed three times with IF buffer (10 min each) to remove the secondary antibody. Sample fixation was done by using 3.7% paraformaldehyde and 0.2% picric acid in KE buffer (50 mM KH2PO4, 5 mM EGTA, pH 5.0) at room temperature for 1 hr. Cross-linking was stopped by using 1X KE buffer containing 0.3M Glycine, followed by two times washing with 1X KE buffer for 1h each. Primary antibodies are mouse monoclonal 8WG16 (ThermoFisherSci,

Waltham, MA) for Pol II RPB1 and anti-GFP polyclonal antibody raised in rabbit (Genscript, Piscataway, NJ). AlexaFluor594 conjugated anti-mouse or anti-rabbit (both from ThermoFisherSci) was used as secondary antibody.

RNA Fluorescence in Situ Hybridization (FISH)

Following IF treatment and fixation, the protoplasts were stored in 70% ethanol at 4°C overnight before FISH steps. The samples were baked onto Superfrost® microscope slides (ThermoFisherSci) at -20°C for 30 minutes, followed by baking at 70°C for 2 hours. Next, the samples were washed with 1X PBS containing 2% bovine serum albumin (BSA), 0.1% cellulase, 0.05% macerozyme, 0.3% Triton X-100, and 0.5% Nonidet P-40 at room temperature for 30 min. Then, samples were washed three times with 100 mM Tris (pH 6.8) containing 1% Nonidet P-40 and 0.5% Triton X-100 at 37°C for 10 minutes each. Pre-chilled methanol with 2% hydrogen peroxide was added to the samples, which were incubated at -20°C for 30 min. The slides were subjected to three rounds of liquid nitrogen treatment, each lasting 5 seconds. The samples were then treated with 0.5% (v/v) Acetic anhydride in 0.1 M triethanolamine (TEA) buffer (pH 8.0) at room temperature for 20 min.

Samples were then blocked with PerfectHyb™ Plus hybridization buffer (ThermoFisherSci) at 55°C for 30 min. Probes (corresponding to the 98-188 and 270-13 positions in PSTVd genome but in the complementary orientation) were synthesized using T3 Maxiscript kit (ThermoFisherSci)(J. Ma et al., 2022). Probes (2.5-5 µg/ml) were denatured by heating at 100°C for 1 minutes, followed by colling on ice. The denatured probes, along with 5 nM ribonucleoside vanadyl complex (Sigma-Aldrich, St. Louis, MO, USA), were added to PerfectHyb™ Plus Hybridization Buffer and applied to samples on slides, followed by incubation at 55°C overnight.

The samples were then rinsed with 2X SSC, washed with 2X SSC containing 50% formamide at 37°C for 30 min, and subsequently washed with 2X SSC and 1X SSC at room temperature for 30 minutes each. 4',6-diamidino-2-phenylindole (DAPI) was added directly to the samples stain (1 µg/ml) for 5 minutes and then rinsed with distilled water. Anti-fade reagent (ThermoFisherSci) was applied to each sample, and the slides were sealed with nail polish.

Microscopy Imaging

Fluorescence signals were obtained by using a Discover Echo Revolve microscope with DAPI, FITC, and TRITC cubes and Leica Stellaris 5 confocal microscope.

Acknowledgments

This work is supported by US National Science Foundation (MCB-1906060, MCB-2350392, and IOS-2410009 to YW). Yunhan Wang is supported by CALS Deans' scholarship from University of Florida. Symbols in Figure 3 are from bioicons.com. We apologize to colleagues whose work was not cited due to the page limits.

References

Chantarachot, T., & Bailey-Serres, J. (2018). Polysomes, Stress Granules, and Processing Bodies: A Dynamic Triumvirate Controlling Cytoplasmic mRNA Fate and Function. *Plant Physiol, 176*(1), 254-269. doi:10.1104/pp.17.01468

Dissanayaka Mudiyanselage, S. D., Ma, J., Pechan, T., Pechanova, O., Liu, B., & Wang, Y. (2022). A remodeled RNA polymerase II complex catalyzing viroid RNA-templated transcription. *PLoS Pathog., 18*(9), e1010850. doi:10.1371/journal.ppat.1010850

Duncan, S., Johansson, H. E., & Ding, Y. (2023). Reference genes for quantitative Arabidopsis single molecule RNA fluorescence in situ hybridization. *J Exp Bot, 74*(7), 2405-2415. doi:10.1093/jxb/erac521

Fang, X., Wang, L., Ishikawa, R., Li, Y., Fiedler, M., Liu, F., . . . Dean, C. (2019). Arabidopsis FLL2 promotes liquid-liquid phase separation of polyadenylation complexes. *Nature, 569*(7755), 265-269. doi:10.1038/s41586-019-1165-8

Huang, T., Guillotin, B., Rahni, R., Birnbaum, K. D., & Wagner, D. (2023). A rapid and sensitive, multiplex, whole mount RNA fluorescence in situ hybridization and immunohistochemistry protocol. *Plant Methods, 19*(1), 131. doi:10.1186/s13007-023-01108-9

Jiang, J., Ma, J., Liu, B., & Wang, Y. (2019). Combining a simple method for DNA/RNA/protein co- purification and Arabidopsis protoplast assay to facilitate viroid research. *Viruses, 11*(4), 324. doi:10.3390/v11040324

Jolly, C., Mongelard, F., Robert-Nicoud, M., & Vourc'h, C. (1997). Optimization of nuclear transcript detection by FISH and combination with fluorescence immunocytochemical detection of transcription factors. *J Histochem Cytochem, 45*(12), 1585-1592. doi:10.1177/002215549704501201

Kubala, M. H., Kovtun, O., Alexandrov, K., & Collins, B. M. (2010). Structural and thermodynamic analysis of the GFP:GFP-nanobody complex. *Protein Sci, 19*(12), 2389-2401. doi:10.1002/pro.519

Ma, B., & Tanese, N. (2013). Combined FISH and immunofluorescent staining methods to co-localize proteins and mRNA in neurons and brain tissue. *Methods Mol Biol, 1010*, 123-138. doi:10.1007/978-1-62703-411-1_9

Ma, J., Dissanayaka Mudiyanselage, S. D., Hao, J., & Wang, Y. (2023). Cellular roadmaps of viroid infection. *Trends Microbiol, 31*(11), 1179-1191. doi:10.1016/j.tim.2023.05.014

Ma, J., Dissanayaka Mudiyanselage, S. D., Park, W. J., Wang, M., Takeda, R., Liu, B., & Wang, Y. (2022). A nuclear import pathway exploited by pathogenic noncoding RNAs. *Plant Cell, 34*(10), 3543-3556. doi:10.1093/plcell/koac210

Meng, C., Zhao, X., & Lao, J. (2018). A modified immunofluorescence in situ hybridization method to detect long non-coding RNAs and proteins in frozen spinal cord sections. *Exp Ther Med, 15*(6), 4623-4628. doi:10.3892/etm.2018.6046

Meyer, C., Garzia, A., & Tuschl, T. (2017). Simultaneous detection of the subcellular localization of RNAs and proteins in cultured cells by combined multicolor RNA-FISH and IF. *Methods, 118-119*, 101-110. doi:10.1016/j.ymeth.2016.09.010

Miao, Y., Chodasiewicz, M., & Fang, X. (2024). Navigating biomolecular condensates in plants from patterns to functions. *Mol Plant, 17*(9), 1329-1332. doi:10.1016/j.molp.2024.08.001

Ortola, B., & Daros, J. A. (2023). Viroids: Non-Coding Circular RNAs Able to Autonomously Replicate and Infect Higher Plants. *Biology (Basel), 12*(2). doi:10.3390/biology12020172

Philips, J. G., Naim, F., Lorenc, M. T., Dudley, K. J., Hellens, R. P., & Waterhouse, P. M. (2017). The widely used Nicotiana benthamiana 16c line has an unusual T-DNA integration pattern including a transposon sequence. *PLoS One, 12*(2), e0171311. doi:10.1371/journal.pone.0171311

Qi, Y., & Ding, B. (2002). Replication of Potato spindle tuber viroid in cultured cells of tobacco and Nicotiana benthamiana: the role of specific nucleotides in determining replication levels for host adaptation. *Virology, 302*(2), 445-456.

Qi, Y., & Ding, B. (2003). Differential subnuclear localization of RNA strands of opposite polarity derived from an autonomously replicating viroid. *Plant Cell, 15*(11), 2566-2577. doi:10.1105/tpc.016576

Sachdeva, G., Garg, A., Godding, D., Way, J. C., & Silver, P. A. (2014). In vivo co-localization of enzymes on RNA scaffolds increases metabolic production in a geometrically dependent manner. *Nucleic Acids Res, 42*(14), 9493-9503. doi:10.1093/nar/gku617

Schneider, F., Sych, T., Eggeling, C., & Sezgin, E. (2021). Influence of nanobody binding on fluorescence emission, mobility, and organization of GFP-tagged proteins. *iScience, 24*(1), 101891. doi:10.1016/j.isci.2020.101891

Sharp, P. A. (2009). The centrality of RNA. *Cell, 136*(4), 577-580. doi:10.1016/j.cell.2009.02.007

Street, L. A., Rothamel, K. L., Brannan, K. W., Jin, W., Bokor, B. J., Dong, K., . . . Yeo, G. W. (2024). Large-scale map of RNA-binding protein interactomes across the mRNA life cycle. *Mol Cell*. doi:10.1016/j.molcel.2024.08.030

Syed, S., & Lim, B. (2024). Multi-labeling Live Imaging to Quantify Gene Expression Dynamics During Drosophila Embryonic Development. *Methods Mol Biol, 2805*, 137-151. doi:10.1007/978-1-0716-3854-5_9

Takeda, R., Zirbel, C. L., Leontis, N. B., Wang, Y., & Ding, B. (2018). Allelic RNA Motifs in Regulating Systemic Trafficking of Potato Spindle Tuber Viroid. *Viruses, 10*(4). doi:10.3390/v10040160

Wang, Y. (2021). Current view and perspectives in viroid replication. *Curr. Opin. Virol., 47*, 32-37. doi:10.1016/j.coviro.2020.12.004

Wang, Y., Qu, J., Ji, S., Wallace, A. J., Wu, J., Li, Y., . . . Ding, B. (2016). A land plant-specific transcription factor directly enhances transcription of a pathogenic noncoding RNA template by DNA-dependent RNA polymerase II. *Plant Cell, 28*(5), 1094-1107. doi:10.1105/tpc.16.00100

Watkins, J. M., & Burke, J. M. (2024). RNase L-induced bodies sequester subgenomic flavivirus RNAs to promote viral RNA decay. *Cell Rep, 43*(9), 114694. doi:10.1016/j.celrep.2024.114694

Xie, D., Chen, M., Niu, J., Wang, L., Li, Y., Fang, X., . . . Qi, Y. (2021). Phase separation of SERRATE drives dicing body assembly and promotes miRNA processing in Arabidopsis. *Nat Cell Biol, 23*(1), 32-39. doi:10.1038/s41556-020-00606-5

Yokoyama, M., Ogawa, M., Nozu, Y., & Hashimoto, J. (1990). Detection of Specific RNAs by in situ Hybridization in Plant Protoplasts. *Plant and Cell Physiology, 31*(3), 403-406. doi:10.1093/oxfordjournals.pcp.a077923

Zhao, L., Fonseca, A., Meschichi, A., Sicard, A., & Rosa, S. (2023). Whole-mount smFISH allows combining RNA and protein quantification at cellular and subcellular resolution. *Nat Plants, 9*(7), 1094-1102. doi:10.1038/s41477-023-01442-9

Figure Legends

Figure 1. An alternative immunofluorescence protocol. Protoplasts from Nicotiana benthamiana 16C were used for testing. GFP5-ER in protoplasts was detected by α-GFP polyclonal primary antibody and Alexa Fluor594-labeled α-Rabbit secondary antibody. α-Rabbit secondary antibody was added to all IF samples. Scale bar, 5 μm.

Figure 2. An optimized RNA FISH protocol for observing potato spindle tuber viroid. Nucleolar-enriched PSTVd detected by Alexa Fluor488-labeled riboprobe. Scale bar, 8 μm.

Figure 3. Schematic workflow of combined IF and FISH.

Figure 4. Combining immunofluorescence (IF) and RNA fluorescent in situ hybridization (FISH) to colocalize PSTVd and RPB1. A) RPB1 is detected by α-RPB1 polyclonal antibody and Alexa Fluor594-labeled α-Rabbit secondary antibody (magenta color).

Secondary antibody was applied to all treatments. PSTVd was detected by Alexa Fluor488-labeled specific riboprobe (green). Probes were added to all treatments. (B) For the image at the bottom right in (A), single channels and RPB1/PSTVd overlay are shown. This image is selected from a Z-stack series. White arrow heads point to some colocalized loci. Scale bar, 5 μm.

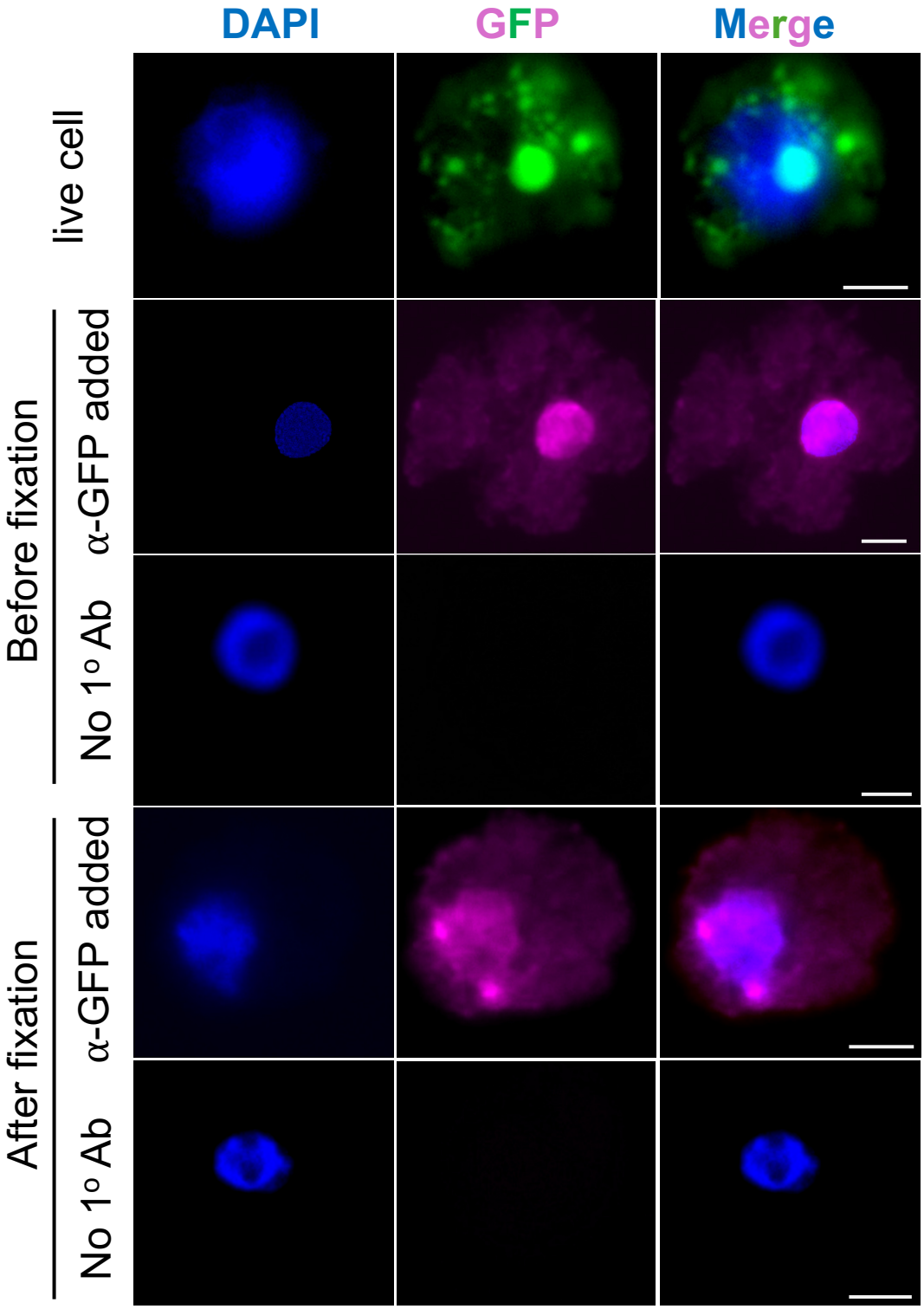
DAPI
GFP
Merge
live cell
Before fixation
No 1° Ab
α-GFP added
After fixation
No 1° Ab
α-GFP added

Figure 1

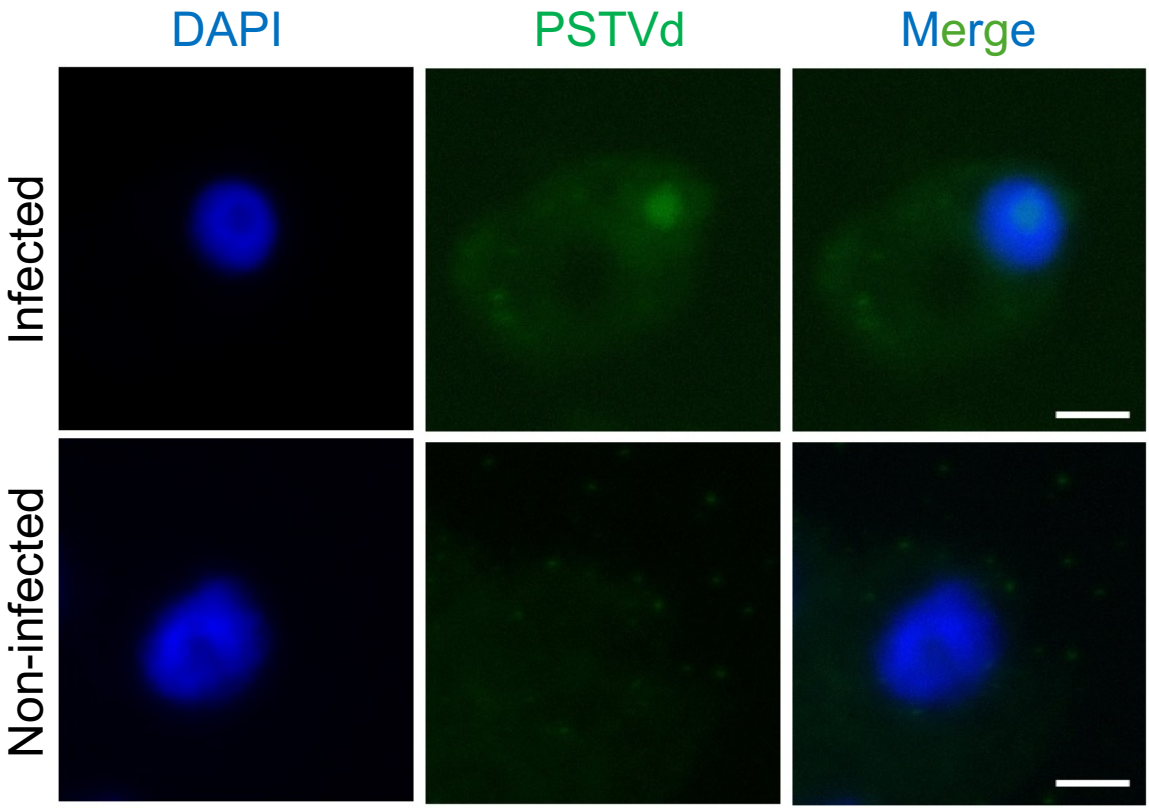

Figure 2

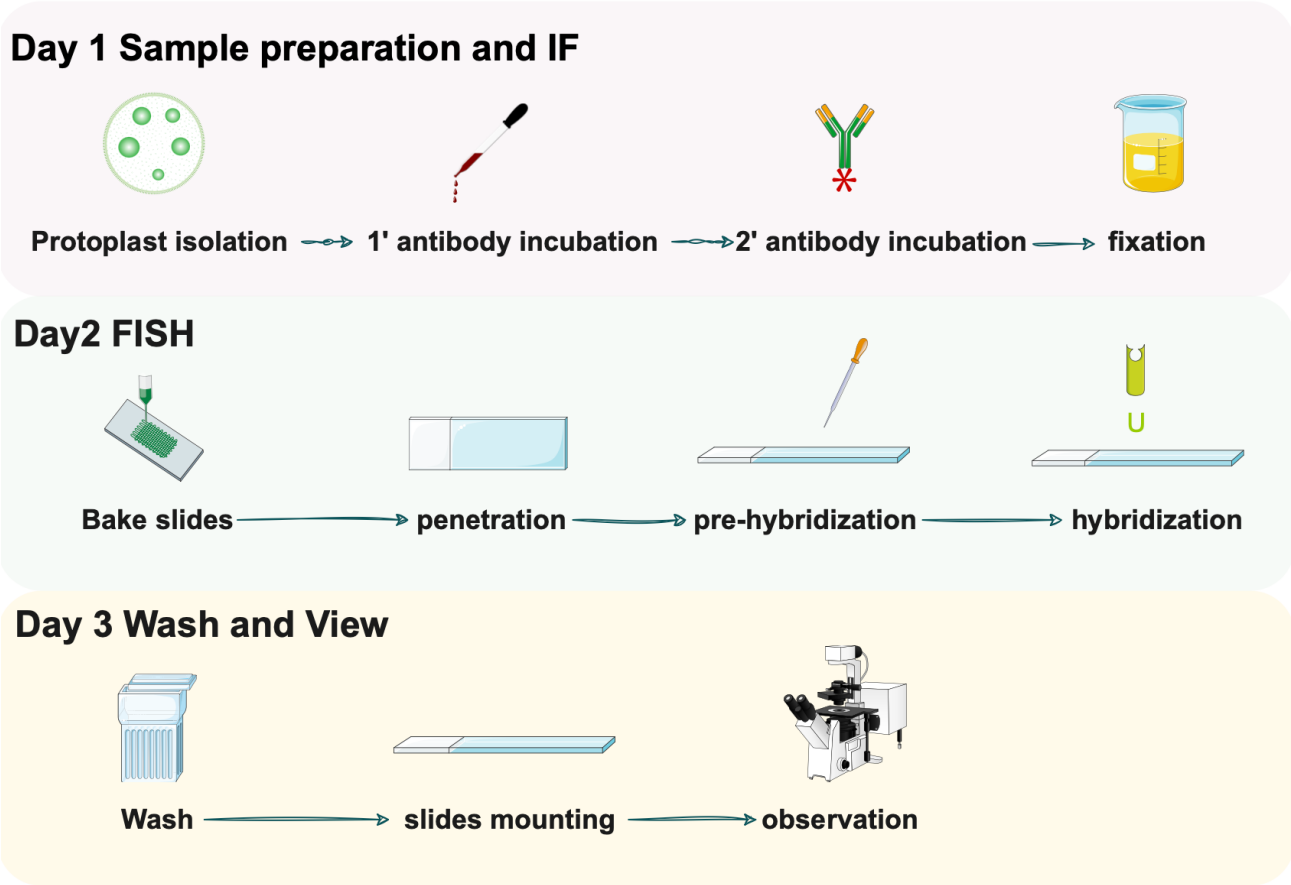
Day 1 Sample preparation and IF
Protoplast isolation
1' antibody incubation
2' antibody incubation
fixation
Day2 FISH
Bake slides
penetration
pre-hybridization
hybridization
Day 3 Wash and View
Wash
slides mounting
observation

Figure 3

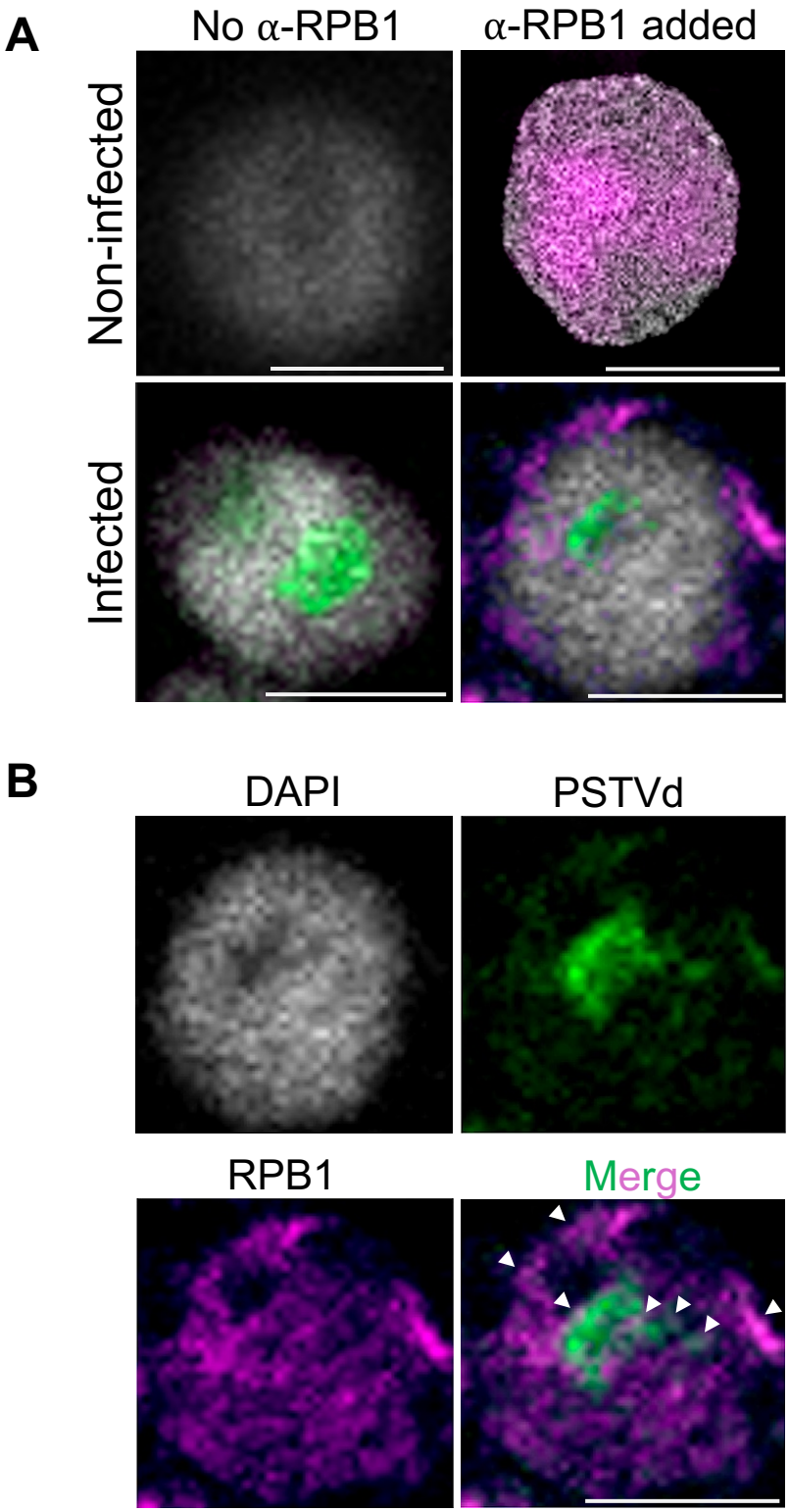
A
No α-RPB1
α-RPB1 added
Non-infected
Infected
B
DAPI
PSTVd
RPB1
Merge

Figure 4